PROGRESS IN COLOR, COLORANTS AND COATINGS

available online @ www.pccc.icrc.ac.ir

Progress in Color Colorants Coating 17 (2024), 227-238

Ministry of Science, Research and Technology
Institute for Color Science & Technology

Multispectral Imaging and Hyperspectral Techniques Applied to Dyed Fibers: a Classification Approach

A. Koochakzaei*[1], B. Jelodarian Bidgoli[1], S. Safapour[2], A. Nemati-Babaylou[1]

[1.] Department of Conservation and Archaeometry, Faculty of Cultural Materials Conservation, Tabriz Islamic Art University, P.O. Box: 51385-4567, Tabriz, Iran

[2.] Key Laboratory of Advanced Eco-Dyeing and Functional Finishing of Textiles, Faculty of Carpet, Tabriz Islamic Art University, P.O. Box: 51385-4567, Tabriz, Iran

ARTICLE INFO

Article history:
Received: 30 June 2023
Final Revised: 11 Nov 2023
Accepted: 13 Nov 2023
Available online: 17 Jan 2024

Keywords:
Spectral imaging
Dye classification
Non-invasive analysis
Mordant
Multivariate analysis

ABSTRACT

This work investigates the possibility of identification of natural dyes (madder and cochineal) and mordant types (Al, Sn, Cr, Cu, Fe) in dyed wool fibers using spectral imaging-based methods. For this purpose, technical imaging, including UVL, IRR and UVR, and obtained IRFC and UVFC images were used, along with multispectral imaging (350-1100 nm) and hyperspectral imaging (400-950 nm). The grayscales of multispectral and hyperspectral images were extracted to quantify the imaging data. The grayscale and the first derivative of the reflectance spectra obtained from the hyperspectral camera were investigated using multivariate principal component analysis and hierarchical clustering to separate the different groups of dyed fibers. According to results, aluminum and tin mordanted fibers could be distinguished from other groups as per UVL and IRFC images; similarly, the type of dye (madder or cochineal) was distinguishable from UVFC images. Interestingly, PCA analysis of grayscales of multispectral images provided an appropriate separation of all groups of fibers with different mordants and dyes. The 3d PCA plot and the hierarchical clustering of the first derivative of the reflectance spectra also resulted in better separation and classification of the dyed fiber groups. Nevertheless, the best performance in clustering fibers groups can be seen in the PCA analysis of grayscales obtained from hyperspectral images recorded at 430-830 nm. Therefore, hyperspectral imaging can be considered a more appropriate method for categorizing dyed fibers with different dyes and mordants. Prog. Color Colorants Coat. 17 (2024), 227-238© Institute for Color Science and Technology.

1. Introduction

Throughout history, humankind has exploited numerous natural sources to dye all kinds of textiles and fabrics using different methods. The selection of dyestuffs is influenced by some variables, such as the type of final product, access to primary dye sources, and cultural, economic, and commercial conditions. Based on these factors, a large volume of various dyed historical textiles and fabrics have remained today in different societies. Examination and identification of the dyeing materials and methods of these artifacts can help evaluating the reasons for the stability of some

*Corresponding author: * a.koochakzaei@tabriziau.ac.ir
alireza.k.1989@gmail.com

https://doi.org/10.30509/pccc.2023.167158.1229

colors over time, the conservation of historical fabrics and using these methods in contemporary dyeing [1].

Red is one of the most important color tones used to dye historical fabrics [2, 3]. This color has been the most popular for all kinds of fabrics and rugs, including Iranian carpets, due to its wide range of applications, high cultural value, and easy access [4-6]. The variety of red dyestuff materials, along with the mordants and various additives, leads to the production of a wide range of colors, which has led to the variety of its use in the production of cultural-artistic works [7, 8]. Most red natural dyes include cochineal, madder, dragon's blood and lac. However, due to their brightness and high hiding power, cochineal and madder are more favoured by craftsmen, and other dyes are often used in combination with these two dyes. Based on traditional instructions, there have been different ways to use these dyes. Usually, depending on the type of fibers, different additives such as alum, iron alum, tin alum, calcium and copper salts have been used to improve color fastness and brightness [7, 9-11].

Identifying the material components of textiles, including fibers, colorants, and mordents, is essential in studying historical artifacts. These data help better understand cultural and economic conditions and business relationships [12]. The organic dyes are usually identified by chromatography methods such as TLC, GC, HPLC, GC/MS, and LC-MS [6, 13-15]. In addition, spectroscopy methods, including Raman, FTIR, and UV-Vis spectrophotometer, are also interesting in identifying the dyes in historical textiles. However, most of these methods require sampling and dye extraction, but this is not always possible due to the limitations and value of historical artifacts. Therefore, non-invasive and portable methods have received more attention in the last two decades. However, applying some of these methods has been limited to preliminary examination and classification of dye/pigments [13-16]. In recent years, the approach to non-invasive examination has turned from spectroscopic methods such as fiber optic reflectance spectroscopy (FORS) and Raman [17-21] to multispectral and hyperspectral imaging methods [21-23]. In addition, using FORS with the development of spectral databases has made the identification process easier and more accurate [24]. It has also made it easier to analyze the reflectance spectra of hyperspectral imaging. On the other hand, multispectral imaging, as a method for primary classification, has effectively identified the colorants remaining in the fibers [25, 26] and provides the possibility of holistic examination along with spot analysis methods. However, most research about the application of imaging methods in the study of colorants in historical and cultural artifacts has been limited to the preliminary investigation of pure dyes and pigments used in paintings or manuscripts [27-29] and less attention has been paid to dyed fibers [23, 30].

On the other hand, the technical studies of dyes in fabrics have mainly focused on identifying colorants. Therefore, investigating other factors affecting the dyeing process, especially the mordants, has received less attention. Mordant identification is generally made using X-ray-based atomic spectroscopy methods, which require sampling and sometimes destroying historical artifacts [31, 32]. Therefore, expanding the use of non-destructive and holistic methods with the ability to identify dyes and mordants simultaneously, which leads to easy, faster and lower-cost identification, is one of the important issues in the study of historical textiles. The most effective strategy would be to use a combination of methods. In this strategy, non-invasive methods are used as a primary method to classify different materials. It leads to the initial classification of all types of samples. On the other hand, it determines the appropriate sampling location based on the study strategy to avoid excessive sampling of valuable artifacts.

Accordingly, considering the effect of dyes and mordants on the spectral characteristics of fibers, methods based on spectral imaging, including technical, multispectral and hyperspectral imaging, can be considered a potential tool for identifying colorants materials in fabrics. Although technical imaging is faster and cheaper than other spectral imaging methods, multispectral and hyperspectral imaging are more accurate.

Therefore, this study aims to expand the efficiency of multispectral, hyperspectral and technical imaging as non-destructive, low-cost methods that can be implemented on-site to identify different dyes and mordant types of dyed fibers. Each method has advantages and capabilities that can be useful in classifying dyed fibers with different mordants in various operational conditions.

2. Experimental

2.1. Mock-up preparation

2.1.1. Mordanting method

In this study, a pre-mordanting method was used. Before mordanting, wool yarns were scoured in a solution containing 5 g/L nonionic detergent at 60 °C for 30 min, and L:R (liquor to good ratio) of 40:1. Then, wool yarns were pre-mordanted in an open beaker using different metal salts such as aluminium sulfate ($Al_2(SO_4)_3.18H_2O$), copper (II) sulfate ($CuSO_4.5H_2O$), iron (II) sulfate ($FeSO_4.5H_2O$), tin (II) chloride ($SnCl_2.2H_2O$), potassium dichromate ($K_2Cr_2O_7$), Merck, Germany. Briefly, 5 g wool yarns were added to the prepared mordant solution at 35 °C, the temperature was raised (2 °C/min) to boil (ca. 93 °C), and mordanting was done for 60 min. Then, the bath was cooled down to 60 °C, and the mordanted samples were removed, rinsed thoroughly with tap water several times to remove unfixed metal cations, dried at room temperature, and used in the dyeing process [33, 34].

2.1.2. Dyeing procedure

Dyeing of raw (unmordanted) and metal mordanted wool yarns with natural dyes (cochineal 20 % owf (on weight of fiber), madder 75 % owf) was carried out at pH=4 (adjusted by glacial acetic acid), using L:R= 40:1. Briefly, the weighed dye powder was added to dyeing bath, boiled for ca. 1 h to extract the dye, and then cooled down to room temperature. Then, the wool samples (raw or metal mordanted, 5 g each) were introduced into the extracted dyed bath at 35 °C; the temperature was raised within 30 min (2 °C/min) to dyeing temperature (boil, ca. 93 °C) and kept at this temperature for 60 min. Next, the dye bath was cooled down to 60 °C, and the dyed samples were removed, thoroughly rinsed with tap water several times to remove unfixed dyes, and air-dried and analyzed [35, 36].

2.2. Methods

2.2.1. Hyperspectral imaging

Hyperspectral Imaging was conducted using the HYSPIM hyperspectral camera model Gamma, which captures information within the 400-950 nm range. Four halogen lamps with a 60-degree angle relative to the sample were used as light sources, and the exposure time was set to 150 ms.

2.2.2. Multispectral imaging (MSI)

All images were captured by the modified camera Nikon D750 after removal of the inbuilt UV-IR blocking filter to exploit the full sensitivity of the CMOS sensor (ca. 350-1100 nm). The camera was equipped with a Nikon AF Nikkor 50 mm f/1.8D lens. The camera was operated in fully manual mode. Following the instructions of Verri and Sanders [37], two electronic xenon flashlights (Youngenu NY660) placed at 45 degrees angle to the subject were used as illuminate sources, and an X-rite ColorChecker was used as a spectral reference to correct images and compare with reference samples. The Lightroom software was used to adjust the white balance of the images using the 18 % grey patch. Following this, the exposure was corrected in the three image channels, with values of 200 for red, green, and blue.

Broadband MSI methods, including Visible-Reflected (VIS), Infrared-Reflected (IR), Ultraviolet-Reflected (UVR) and Ultraviolet-induced Visible Luminescence (UVL) were recorded in RAW format and the highest resolution (24MP: 6016×4016 pixel) using the filters described in Table 1. Multiband spectral imaging was also performed using the 55-85 nm filters shown in Figure 1. Raw images obtained from the camera were converted into 16-bit TIF format in Adobe Photoshop software. Post-processing and calibration procedures were performed according to the Kushel method [38] and Cosentino recommendations [39]. False-color infrared (IRFC) and false-color ultraviolet (UVFC) images were obtained by combining VIS with IR and UVR images, respectively, based on the method proposed by Dyer et al. [40]. The false color technique combines the RGB visible image channel with the reflected image. The IRFC method replaces the R and G channels in the visible image with the G and B channels, respectively, and then replaces the black and white IR image with the R channel to produce an IR-R-G final image. The UVFC method replaces the G and B channels in the visible image with the R and G channels, respectively, and then replaces the black and white UVR image with the B channel, resulting in a G-B-UV final image.

Table 1: Summary of radiation sources and filters used for each imaging method.

Broadband MSI Technique	Filter(s) in front of Radiation Sources	Filter(s) in front of camera	Range investigated
Visible-Reflected imaging (VIS)	2 × Youngenu NY660 Xenon flashlight, each mounted with soft box (without filter)	Baader UV/IR Cut	420-680 nm
Ultraviolet-induced Visible Luminescence imaging (UVL)	+2 × Hoya U-360	Baader UV/IR Cut	420-680 nm
Infrared-Reflected imaging (IR)	2 × Youngenu NY660 Xenon flashlight, each mounted with soft box (without filter)	GREEN.L IR 720 Schott RG830 Zomei 950	720-1100 nm 830-1100 nm 980-1100 nm
Ultraviolet-Reflected imaging (UVR)	+2 × Hoya U-360	Baader U-Venus	350-380 nm

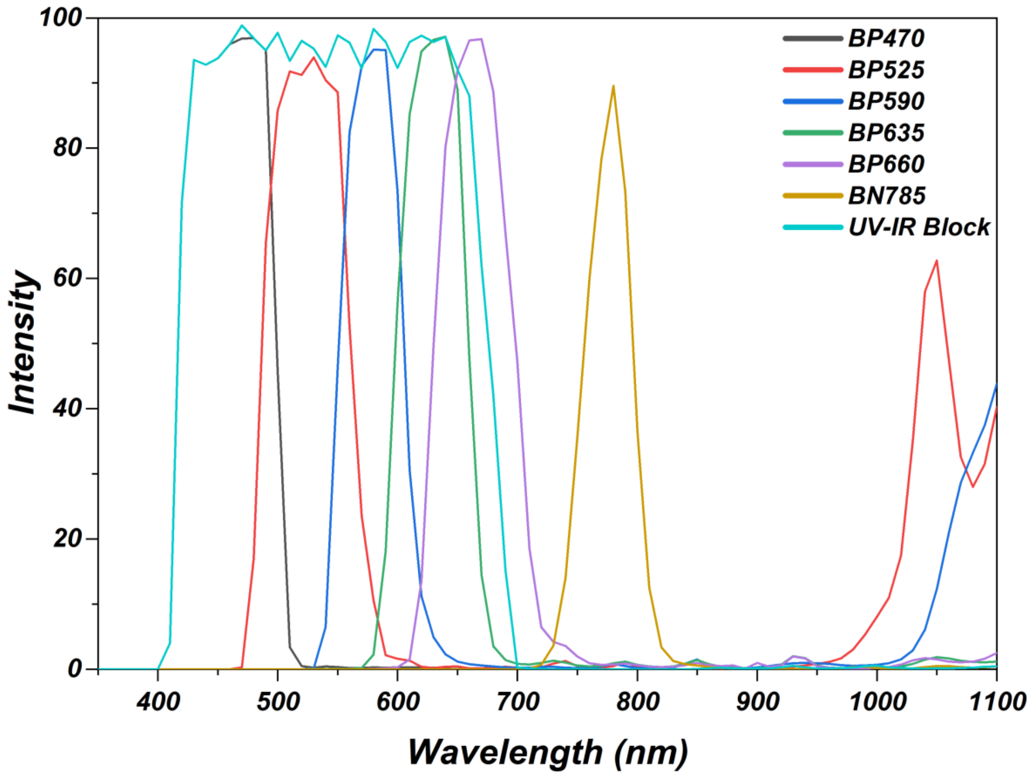

Figure 1: Transmission spectra of Baader UV/IR-Cut/L, Midopt BP470, Midopt BP 525, Midopt BP 590, Midopt BP 635, Midopt BP 660 and Midopt BN785 band-pass glass filters.

The analysis of reflectance spectra was performed using the Originpro2021 software. After smoothing and normalization to the 0-1 range, spectra' first derivatives were obtained. The Savitzky-Golay filter was employed with window points 30 and a polynomial order of 5 to smoothen the data. The identical approach with window point 20 was used to smooth and minimize noise to obtain the derivative spectra. The first derivatives were analyzed using multivariate analyzes, including Principal Component Analysis (PCA) and hierarchical clustering. In PCA, three principal components were extracted, and the discriminatory power of different components in three dimensions was assessed using a correlation matrix. In addition to the reflectance spectra, hyperspectral and multispectral images recorded at different wavelengths were also investigated using principal component analysis. Quantitative data from these images were obtained by measuring the Mean Gray Value by ImageJ software.

3. Results and Discussion

3.1. Technical and multispectral imaging

The results of technical imaging are presented in Figure 2. The UVL images can usually be used to distinguish the origin of the red color in works of art. In this method, organic base dyes have luminescence properties that are not found in other dyes. Previous studies reported light pink and dark red luminescence for madder and cochineal red dyes [41]. What is clear is the difference in luminescence observed in the fibers with different mordants compared to the previous report [41]. Although the substrate, preparation method, and mordant type affect the intensity and color of the luminescence [42], only the specimens mordanted with aluminium and tin, which produce a brighter red color in the fibers, have a red luminescence. Fibers mordanted with copper, chromium and iron, which are darker red, do not show any luminescence. Dark red colors emit weaker luminescence intensity due to higher UV absorption [25].

UVFC images were a good indicator of separating cochineal and madder dyes. In UVFC images, cochineal and madder are usually seen in green and brown color shades, respectively. Separation based on these images is easier on mordanted fibers with tin and aluminium. Madder-dyed fibers, mordanted with aluminium and tin, and cochineal-dyed fibers, mordanted with tin, are yellow in IRFC images. However, cochineal-dyed fibers with aluminium mordant have created an orange tint in IRFC images, which can be considered an indicator of this sample. But in other samples, an orange-red color is generally observed, which cannot be separated. So, we can say that the mordant significantly affects the colors observed in technical imaging. Previous studies have also shown that madder and cochineal, without the mordant on the paper substrate, produce red-orange in IRFC images and red-brown and green in UVFC images, respectively [43-45]. However, madder with aluminium mordant on silk fibers causes yellow and brown in IRFC and UVFC images, respectively, but iron mordant causes orange in IRFC and no luminescence in UVL [24].

Multispectral images are presented in Figure 3a. These images show grey shades; at first sight, it is impossible to separate them qualitatively. Nevertheless, the images recorded at 660-590 nm wavelengths make separating tin and aluminium mordanted fibers possible due to different absorption and higher reflectance.

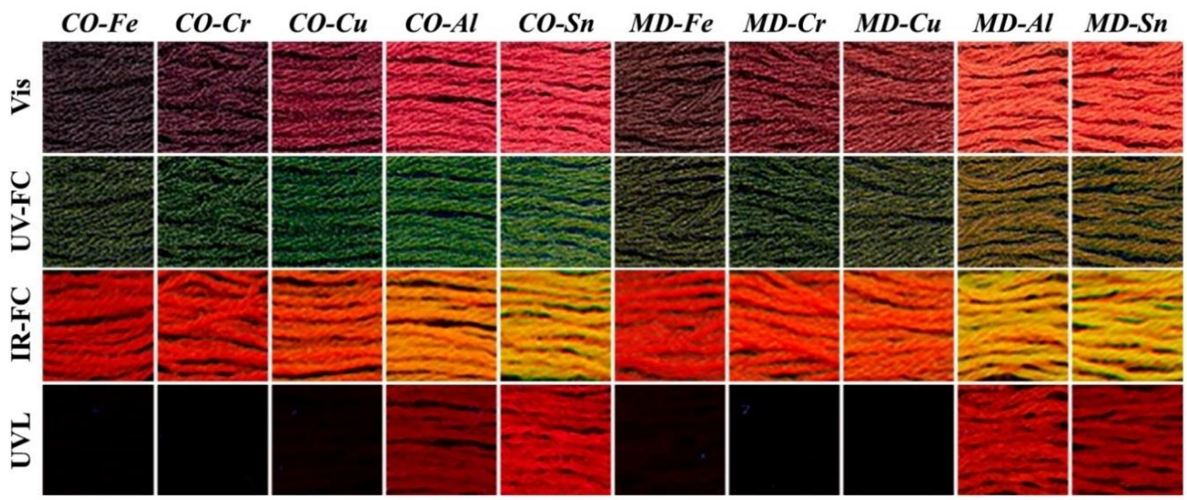

Figure 2: Technical images including visible, UV-FC, IRFC and UVL images of fiber dyed with cochineal (CO) and madder (MD), mordanted with different materials.

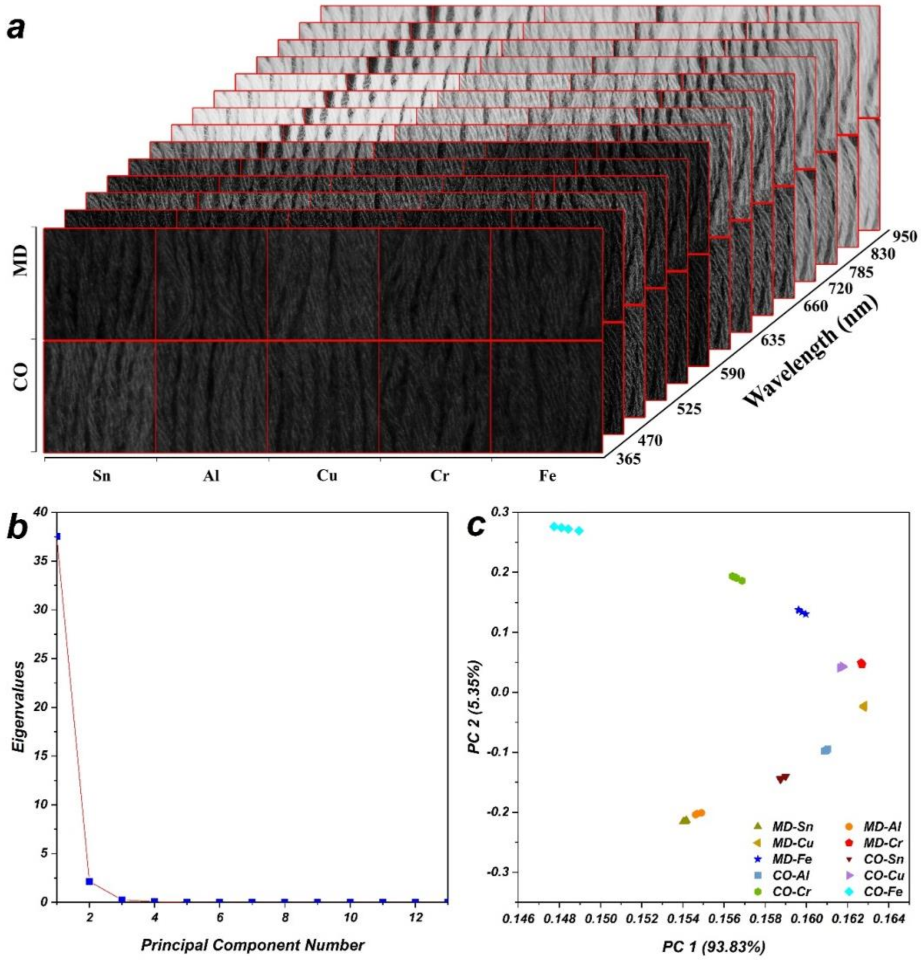

Figure 3: a: Multispectral images recorded of fibers dyed with madder (MD) and cochineal (CO) in the wavelength range of 350-1110 nm; b: scree plot of grayscale data obtained from multispectral images, which shows the sufficiency of two principal components to analyze the data using the PCA method; c: PCA score plot of two components, PC1 and PC2, which show the proper separation of dyed fiber groups based on grayscale values.

However, the quantitative examination of data provides better classification than the images. Therefore, the reflection intensity was calculated based on the grayscale values of multispectral images. Grayscale allows the quantitative examination of brightness changes in these images. The logarithm of grayscale values was investigated using PCA analysis. The scree plot shows that the eigenvalues form a straight line after the second principal component. Therefore, PC1 and PC2, with 93.83 and 5.35 % of the variance, are sufficient for data analysis. The PC1-PC2 score plot resulting from the principal component analysis of grayscale logarithms is presented in Figure 3c. What is clear is the capability of the grayscale values of multispectral images in classifying fibers with different dyes and mordants. Also, the results show that aluminium and tin mordants produce relatively similar color shades in the fibers dyed with madder. This phenomenon can also be observed in the fibers dyed with madder with chrome mordant and red cochineal with copper mordant.

3.2. Hyperspectral imaging

To separate samples using hyperspectral imaging, images recorded in different wavelengths were used along with reflectance spectra. The reflectance spectra of different samples are presented in Figure 4a. The most significant difference between the spectra is observed at 550 to 850 nm. The first spectra derivative was calculated to investigate better the minor differences in the spectra (Figure 4b). Derivative spectrophotometry enhances the ability to detect spectral features by improving resolution, eliminating background interference, and creating distinct fingerprints [46].

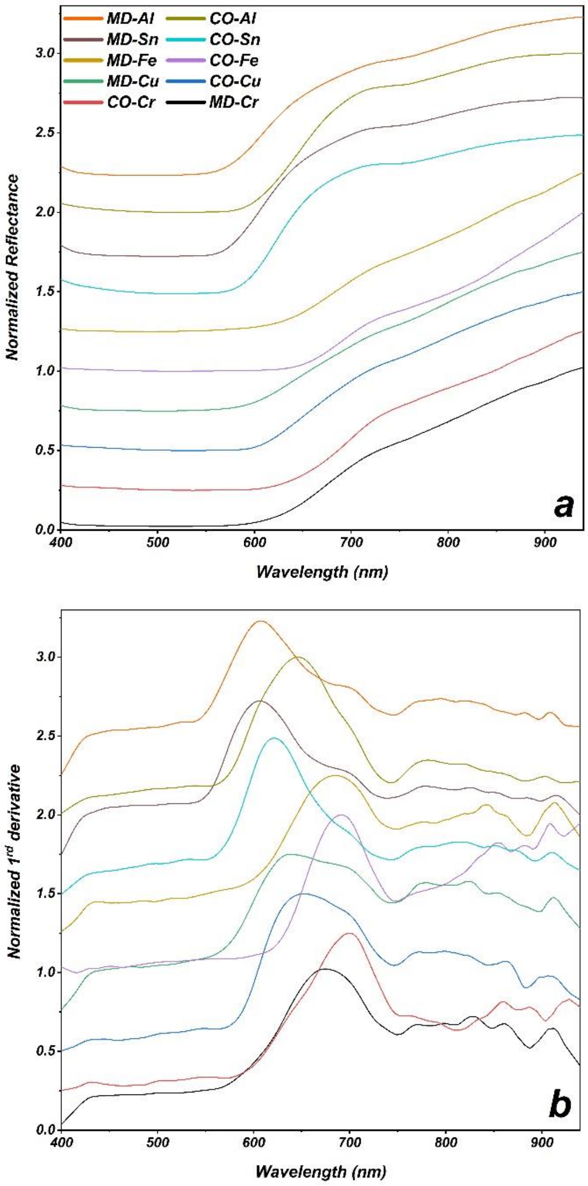

Figure 4: Hyperspectral reflectance spectra in the range of 400-950 nm (a) and their first derivative (b).

An experiment was conducted using this method to study the dyeing process of Iranian carpet wool yarns with varying amounts of dyes derived from different types of madder, yielding more accurate outcomes than the initial spectra [47]. As seen in Figure 4, the essential difference of the spectra's first derivative is at 550 to 750 nm. However, due to slight differences below 500 nm and the NIR range, the normalized data of the whole spectrum derivative was used for multivariate analysis.

According to the PCA analysis of the first derivative of spectra, the first (69.35 % variance), second (25.77 % variance), and third (2.73 % variance) components are sufficient to evaluate the data. For this reason, the first three principal components, including 97.49 % of the variance, were examined in the three-dimensional PCA plot presented in Figure 5a. These three main components made it possible to separate all the dyed fibers with different dyes and mordants. Although the percentage of variance for PC3 is low, this principal component has helped to separate the samples better. In addition to PCA, hierarchical clustering analysis was also performed on the first derivative of the spectra, which can be seen in Figure 5b. In this analysis, the dyed fibers were placed in 10 separate clusters. Similar to the findings from multispectral imaging, hierarchical clustering analysis reveals the minimum distance between the madder-dyed fibres mordanted with aluminium and tin based on the reflection spectra. In fact, aluminium and tin mordants seem to cause very close color spectra in the dyeing of wool fibers using madder.

Figure 6 shows the recorded hyperspectral images of fibers at wavelengths 430, 580, 600, 630, 680, 730, 800 and 830 nm. These wavelengths were selected due to observing different reflection intensities of the dyed fibers. Examining these images shows the possibility of separating madder-dyed fibers with a tin mordant at 430 nm. At 580 nm, it is possible to see the separation of the cochineal dyed fibers with aluminium and tin mordants due to higher reflectance than other fibers. However, it is impossible to distinguish the tin and aluminium mordanted cochineal-dyed fibers in this Figure. Also, copper-mordanted fibers, both in dyeing with cochineal and madder, show the lowest amount of reflection. But in general, separating the dyed fibers based only on the qualitative description of the images is not easy. Therefore, for a quantitative review of the results, the grayscale value was calculated for images recorded in different wavelengths, and their logarithm was analyzed by the PCA method. Accordingly, the 3D PCA plot, based on PC1 (78.78 % of the total variance), PC2 (17.08 % of the total variance) and PC3 (3.91 % of the total variance), is presented in Figure 6. Examining this plot shows the possibility of separating all the investigated fibers groups and the significant correlation of the samples of each group. In addition to the possibility of separating fibers based on the type of dye, hyperspectral imaging provides the opportunity for separation based on the mordants used in the dyeing process. This separation can be done based on the reflective spectra or the grayscale values obtained from the recorded images at different wavelengths.

In addition, utilizing the results obtained from technical and hyperspectral imaging conducted at different wavelengths makes it feasible to put forward the flowchart illustrated in Figure 7 as a viable approach for effectively discerning and distinguishing between a wide range of diverse samples.

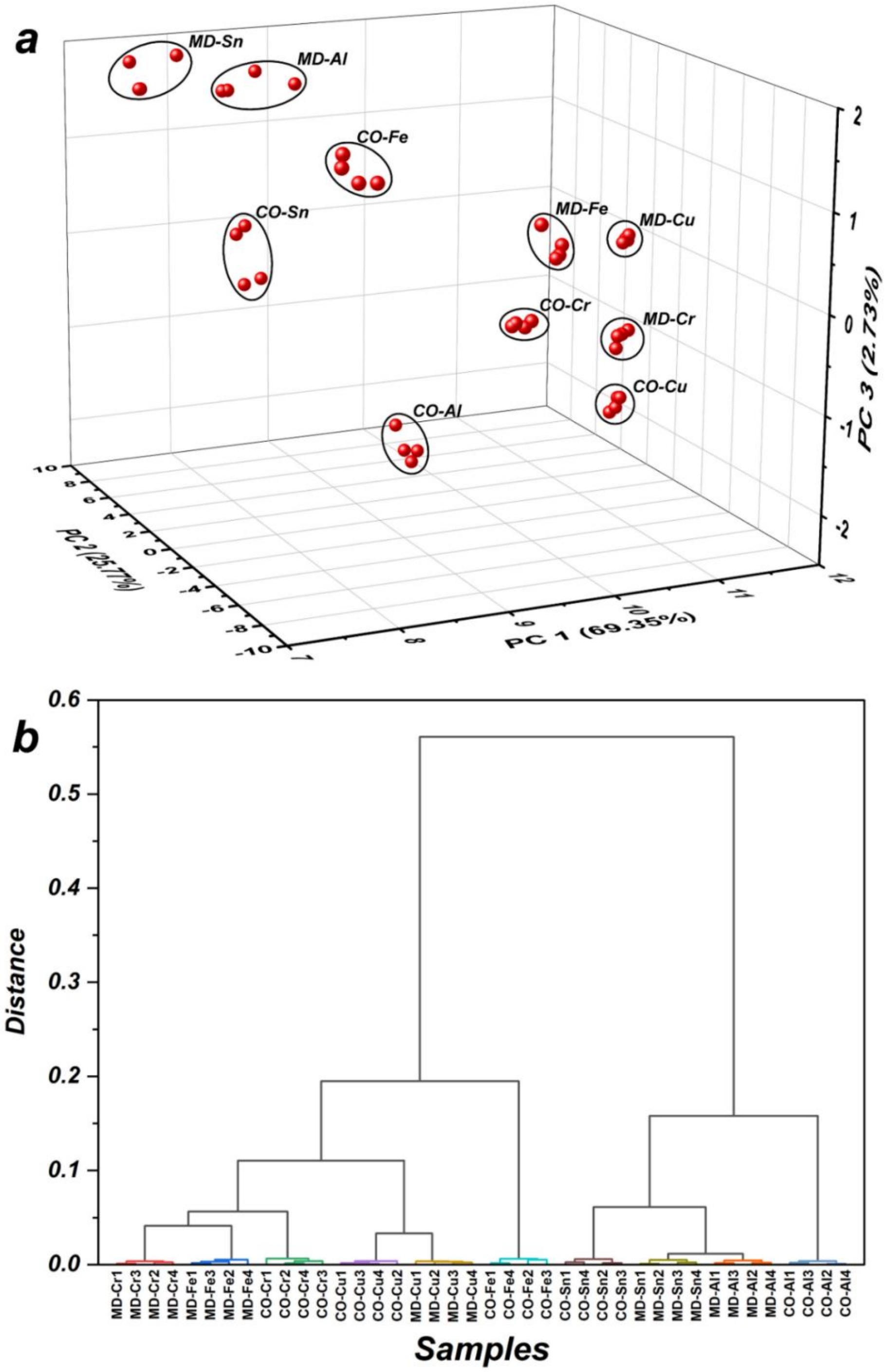

Figure 5: 3D PCA score plot (a) and hierarchical clustering (b) derived from the first derivative of the Hyperspectral reflectance spectra after normalization between 0-1.

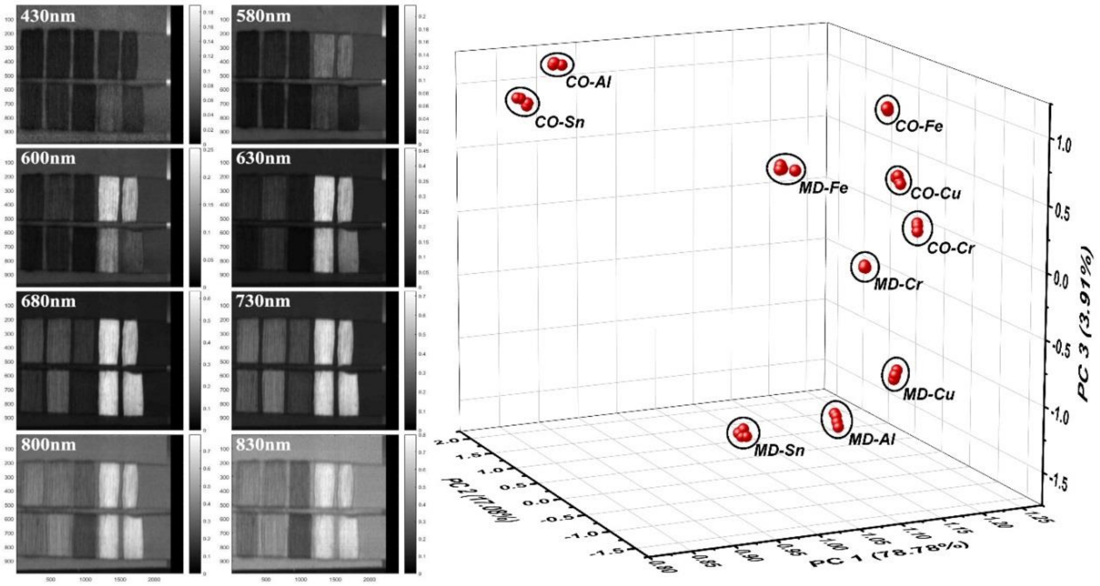

Figure 6: Hyperspectral images in various wavelengths that showed different reflections of the dyed fibers (left) and a 3D Score plot of PCA analysis of logarithms of grayscale values obtained from the hyperspectral images that show the separation of dyed fibers groups (right).

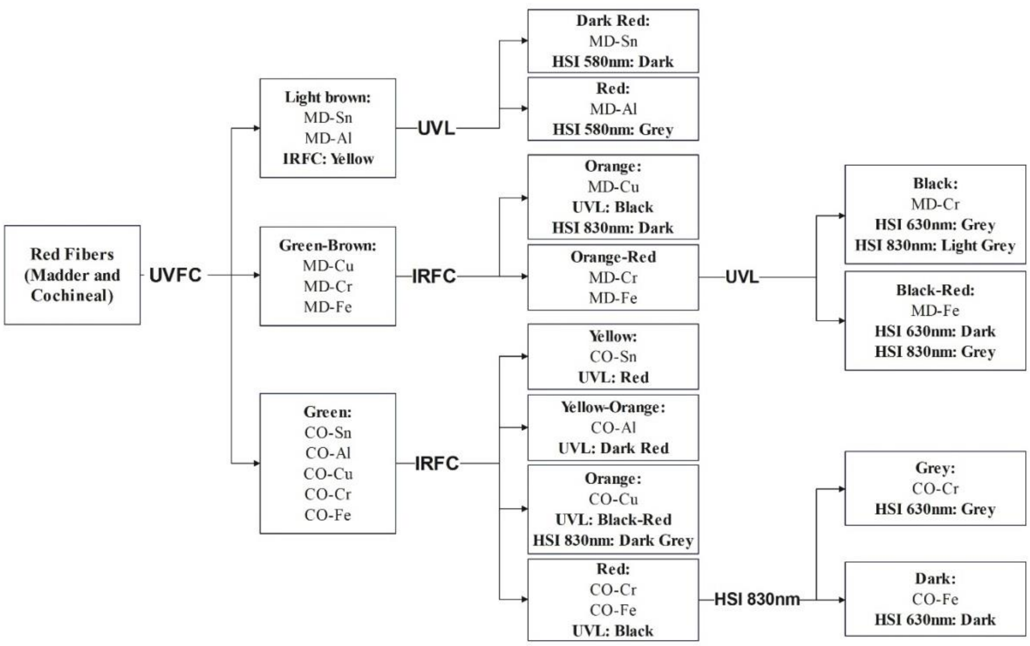

Figure 7: The Proposed flowchart for separating dyed fibers with madder and cochineal, with different mordants, based on the technical and hyperspectral imaging results.

4. Conclusion

The possibility of classification of wool fibers dyed in different conditions, i.e., natural dyes (cochineal and madder) and mordants (Al, Sn, Cr, Cu, and Fe) were investigated based on spectral imaging such as technical, multispectral and hyperspectral imaging, Principal Component Analysis (PCA) and Hierarchical Clustering. Although, madder and cochineal are usually reported with rose pink and dark red luminescence in UVL images, respectively, our results showed that the observed luminescence is influenced by the type of mordants used in dyeing. In this study, only the mordanted fibers with aluminium and tin exhibit red luminescence. In contrast, no luminescence was observed in fibers mordanted with copper, chromium and iron. This matter can be due to more UV absorption in these samples due to their darker final color. In the UVFC images, cochineal and madder are observed with green and brown colors, respectively. Thus, UVFC is a suitable method for classifying cochineal from madder. Also, the IRFC images can distinguish the aluminium and tin-mordanted fibers from other dyed fibers.

Due to different absorption and more reflection, it was also possible to distinguish aluminium and tin-mordanted samples from others via multispectral images (in the range of 590-660 nm). The two-dimensional PCA plot of PC1 and PC2 from the data related to the grayscale of the multispectral recorded images showed an acceptable separation of the fibers dyed with madder and cochineal with different mordants. Therefore, the results show the ability of this method to separate wool fibers dyed in different conditions.

In addition, the results from hyperspectral imaging (examining reflective spectra and examining images recorded at different wavelengths) through evaluation of the first derivative of the reflectance spectrum using the PCA test and Hierarchical Clustering showed the appropriate resolution of all groups of fibers with different dyes and mordants. As per hyperspectral images, different dyes and mordants resulted in different reflections at wavelengths of 430, 580, 600, 630, 680, 730, 800, and 830 nm. Subsequently, the grayscale of hyperspectral images was examined by PCA method. 3D PCA plot showed the best performance for classification in different groups of dyed fibers.

The results of this study show that if a suitable database is created, the spectral imaging methods would perform well in the separation and identification of fibers dyed in different conditions. This method, especially in large collections of historical textiles, will help reduce examination time, costs, and initial grouping of samples. It is noteworthy that looking at several variables requires establishing an extensive database to analyze multiple variables. Future research should include the evaluation of various concentrations and mixtures of dyes and mordants and the effects of aging.

5. References

1. Landi S. Textile conservator’s manual. Oxfordshire: Routledge; 2012.
2. Phipps E. Cochineal Red: The Art History of a Color. The Metropolitan Museum of Art Bulletin. 2010;67(3).
3. Sandberg G. The Red Dyes: Cochineal, Madder, and Murex Purple: a World Tour of Textile Techniques. North Carolina: Lark Books; 1996.
4. Savory R, Dhamija J, Ittig A, Sherrill SB, Rubinson KS, Schimtz B, et al. CARPETS. Encyclopaedia Iranica Online: Brill. p. 834-90;1-9.
5. Brunello F. The Art of Dyeing in the History of Mankind. North Carolina: American Association of Textile Chemists and Colorists; 1973.
6. Koochakzaei A, Sarhaddi-Dadian H, Oudbashi O, Achachluei MM, Moradi H. Parthian dyed fabric discovered from Kuh-e Khwaja archaeological site, Sistan, Iran: A multi-analytical study for dye identification. J Archaeological Scie: Rep. 2023; 52:104288. https://doi.org/10.1016/j.jasrep.2023.104288.
7. Wulff HE, Technology MIo. The Traditional Crafts of Persia: Their Development, Technology, and Influence on Eastern and Western Civilizations. Massachusetts: M.I.T. Press; 1966.
8. Hosseinnezhad M, Gharanjig K, Jafari R, Imani H. Green dyeing of woolen yarns with weld and madder natural dyes in the presences of biomordant. Prog Color Colorants Coat. 2021; 14(1):35-45. https://doi.org/10.30509/pccc.2021.81678.
9. Cardon D. Natural Dyes: Sources, Tradition, Technology and Science. London: Archetype; 2007.
10. Bagherzadeh Kasiri M, Safapour S. Exploring and exploiting plants extracts as the natural dyes/antimicrobials in textiles processing. Prog Color Colorants Coat. 2015; 8(2):87-114. https://doi.org/10.30509/pccc.2015.75856.
11. Sadeghi-Kiakhani M, Safapour S, Golpazir Y. Impact of chitosan-poly(amidoamine) dendreimer hybrid treatment on dyeing and color fastness properties of wool yarn with madder natural dye. Prog Color Colorants Coat. 2019; 12(4):241-50. https://doi.org/10.30509/pccc.2019.81595.
12. Koochakzaei A, Achachluei MM, Mehrabad MS. Identification of fibers and weaving technology in the remains of fabrics discovered from Kuh-e Khwaja, A Parthian Archaeological Site in Sistan, Iran. J Ancient History Archaeol. 2021; 8(3). https://doi.org/10.1016/j.jasrep.2023.104288.
13. Shahid M, Wertz J, Degano I, Aceto M, Khan MI,

Quye A. Analytical methods for determination of anthraquinone dyes in historical textiles: A review. Analy Chim Acta. 2019; 1083:58-87. https://doi.org/10.1016/j.aca.2019.07.009.

14. Degano I, Ribechini E, Modugno F, Colombini MP. Analytical methods for the characterization of organic dyes in artworks and in historical textiles. Appl Spect Rev. 2009; 44(5):363-410. https://doi.org/10.1080/05704920902937876.
15. Rosenberg E. Characterisation of historical organic dyestuffs by liquid chromatography–mass spectrometry. Anal Bioanal Chem. 2008; 391(1):33-57. https://doi.org/10.1007/s00216-008-1977-0
16. Gulmini M, Idone A, Diana E, Gastaldi D, Vaudan D, Aceto M. Identification of dyestuffs in historical textiles: Strong and weak points of a non-invasive approach. Dyes Pigm. 2013; 98(1):136-45. https://doi.org/10.1016/j.dyepig.2013.02.010.
17. Maynez-Rojas MA, Casanova-González E, Ruvalcaba-Sil JL. Identification of natural red and purple dyes on textiles by Fiber-optics Reflectance Spectroscopy. Spectrochim Acta Part A: Mol Biomol Spect. 2017;178:239-50. https://doi.org/10.1016/j.saa.2017.02.019.
18. de Ferri L, Tripodi R, Martignon A, Ferrari ES, Lagrutta-Diaz AC, Vallotto D, Pojana G. Non-invasive study of natural dyes on historical textiles from the collection of Michelangelo Guggenheim. Spectrochim Acta Part A: Mol Biomol Spect. 2018; 204:548-67. https://doi.org/10.1016/j.saa.2018.06.026
19. Smith GD, Esson JM, Chen VJ, Hanson RM. Forensic dye analysis in cultural heritage: Unraveling the authenticity of the earliest Persian knotted-pile silk carpet. Forensic Science International: Synergy. 2021; 3:100130.
20. Fonseca B, Schmidt Patterson C, Ganio M, MacLennan D, Trentelman K. Seeing red: towards an improved protocol for the identification of madder- and cochineal-based pigments by fiber optics reflectance spectroscopy (FORS). Heritage Science. 2019; 7(1):92. https://doi.org/10.1186/s40494-019-0335-1
21. Koochakzaei A, Oudbashi O. A courtly brocade belt belonging to Qajar period (1789–1925), Iran. Heritage Science. 2023; 11(1):29.
22. Webb EK, Summerour R, Giaccai J. A case study using multiband & hyperspectral imaging for the identification & characterization of materials on archaeological andean painted textiles. Textile Group Postprints. Washington, DC: AIC; 2014. p. 23–36.
23. Peruzzi G, Cucci C, Picollo M, Quercioli F, Stefani L. Non-invasive identification of dyed textiles by using VIS-NIR FORS and hyperspectral imaging techniques. Cultura e Scienza del Colore - Color Culture Sci. 2021;13(01):61-9. https://doi.org/10.23738/CCSJ.130207.
24. Tamburini D, Dyer J. Fibre optic reflectance spectroscopy and multispectral imaging for the non-invasive investigation of Asian colourants in Chinese textiles from Dunhuang (7th-10th century AD). Dyes Pigm. 2019; 162:494-511. https://doi.org/10.1016/j.dyepig.2018.10.054
25. Dyer J, Tamburini D, O'Connell ER, Harrison A. A multispectral imaging approach integrated into the study of Late Antique textiles from Egypt. PLOS ONE. 2018; 13(10):e0204699. https://doi.org/10.1371/journal.pone.0204699
26. Tamburini D, Dyer J, Davit P, Aceto M, Turina V, Borla M, et al. Compositional and micro-morphological characterisation of red colourants in archaeological textiles from pharaonic Egypt. Molecules. 2019; 24(20). https://doi.org/10.3390/molecules24203761.
27. Cosentino A. Identification of pigments by multispectral imaging; a flowchart method. Herit Sci. 2014; 2(1):8. https://doi.org/10.1186/2050-7445-2-8
28. Daveri A, Vagnini M, Nucera F, Azzarelli M, Romani A, Clementi C. Visible-induced luminescence imaging: A user-friendly method based on a system of interchangeable and tunable LED light sources. Microchem J. 2016; 125:130-41. https://doi.org/10.1016/j.microc.2015.11.019.
29. Koochakzaei A, Ghaffari T. Identification of traditional black Persian inks by spectroscopic and spectral imaging techniques: Presenting a flowchart method. Vibrat Spect. 2023; 127:103545. https://doi.org/10.1016/j.vibspec.2023.103545.
30. Rahaman GMA, Parkkinen J, Hauta-Kasari M. A novel approach to using spectral imaging to classify dyes in colored fibers. Sensors. 2020; 20(16). https://doi.org/10.1016/j.vibspec.2023.103545.
31. Al-Sharairi N, Sandu ICA, Vasilache V, Sandu I. Recognition of natural silk fibers, dyes and metal threads of historical Romanian textile fragments using the multi-analytical techniques approach. Text Res J. 2020; 90(15-16):1671-88. https://doi.org/10.1177/0040517519898827
32. Indictor N, Koestler RJ, Sheryll R. The detection of mordants by energy dispersive X-ray spectrometry: Part I. dyed woolen textile fibers. J Am Inst Conserv. 1985; 24(2):104-9. https://doi.org/10.2307/3179451.
33. Safapour S, Rather LJ, Mazhar M. Coloration and functional finishing of wool via prangos ferulacea plant colorants and bioactive agents: colorimetric, fastness, antibacterial, and antioxidant studies. Fiber Poly. 2023; 24(4):1379-88. https://doi.org/10.1007/s12221-023-00156-1
34. Safapour S, Rather LJ, Mir SS, Dar QF. Upscaling Millettia laurentii carpentry sawdust into natural dyes: imparting antimicrobial, antioxidant, and UV-protective finish to wool yarns through an ecological and sustainable natural dyeing process. Biomass Conv Bioref. 2023. https://doi.org/10.1007/s13399-023-04184-y
35. Safapour S, Mazhar M, Abedinpour S. Color shade extension of reseda luteola L. natural colorant on wool textiles via binary combination of metal salts: colorimetric and fastness studies. Fiber Poly. 2023;

24(9):3221-33. https://doi.org/10.1007/s12221-023-00296-4.

36. Safapour S, Rather LJ, Safapour R, Mir SS. Valorization of bio-colorants extracted from Hypercium scabrum L. plant for sustainable and ecological coloration of wool yarns. Heliyon. 2023; 9(9):e19439. https://doi.org/10.1016/j.heliyon.2023.e19439
37. Verri G, Saunders D. Xenon flash for reflectance and luminescence (multispectral) imaging in cultural heritage applications. British Museum Tech Res Bull. 2014; 8:83-92.
38. Kushel D. Photographic Techniques. In: Frey FS, editor. The AIC guide to digital photography and conservation documentation. Third ed ed: American Institute for Conservation of Historic and Artistic Works; 2017.
39. Cosentino A. Practical notes on ultraviolet technical photography for art examination. Notas práticas sobre a fotografia de ultravioleta para o exame de obras de arte. 2015; 21:53-62.
40. Dyer J, Verri G, Cupitt J. Multispectral Imaging in Reflectance and Photo-induced Luminescence modes: A User Manual: British Museum; 2013.
41. de la Rie ER. Fluorescence of paint and varnish layers (Part 1). Studies in Conservation. 1982; 27(1):1-7.
42. Derrick M, Newman R, Wright J. Characterization of yellow and red natural organic colorants on Japanese woodblock prints by EEM fluorescence spectroscopy. J Am Inst Conserv. 2017; 56(3-4):171-93. https://doi.org/10.1080/01971360.2016.1275438
43. Villafana T, Edwards G. Creation and reference characterization of Edo period Japanese woodblock printing ink colorant samples using multimodal imaging and reflectance spectroscopy. Herit Sci. 2019; 7(1):94. https://doi.org/10.1186/s40494-019-0330-6.
44. Koochakzaei A, Alizadeh Gharetapeh S, Jelodarian Bidgoli B. Identification of pigments used in a Qajar manuscript from Iran by using atomic and molecular spectroscopy and technical photography methods. Herit Sci. 2022; 10(1):30. https://doi.org/10.1186/s40494-022-00665-x.
45. Koochakzaei A, Mobasher Maghsoud E, Jelodarian Bidgoli B. Non-invasive imaging and spectroscopy techniques for identifying historical pigments: a case study of Iranian manuscripts from the Qajar era. Herit Sci. 2023;11(1):157. https://doi.org/10.1186/s40494-023-01011-5
46. Ghanean S, Ghanbar Afjeh M. Application of the nondestructive second derivative spectrophotometry to eliminate the effect of substrate in identification of madder used in Persian carpets. Color Res Appl. 2018; 43(2):238-46. https://doi.org/10.1002/col.22182
47. Ghanean S, Ghanbar Afjeh M. Application of derivative spectrophotometry to determine the relation between color intensity and dye concentration of madder. Prog Color Colorant Coat. 2016; 9(3):183-94. https://doi.org/10.30509/pccc.2016.758

How to cite this article:
Koochakzaei A, Jelodarian Bidgoli B, Safapour S, Nemati-Babaylou A. Multispectral Imaging and Hyperspectral Techniques Applied to Dyed Fibers: a Classification Approach. Prog Color Colorants Coat. 2024;17(3):227-238. https://doi.org/10.30509/pccc.2023.167158.1229